Published in final edited form as:
Mol Cancer Ther. 2009 August ; 8(8): 2441–2451. doi:10.1158/1535-7163.MCT-09-0113.

HYD1-induced increase in ROS leads to autophagy and necrotic cell death in multiple myeloma cells

Rajesh R. Nair[1,*], **Michael F. Emmons**[1,*], **Anne E Cress**[2], **Raul F. Argilagos**[1], **Kit Lam**[3], **William T. Kerr**[4], **Hong-Gong Wang**[5], **William S. Dalton**[6], and **Lori A. Hazlehurst**[1,6]

[1]Molecular Oncology Program, Moffitt Cancer Center, Tampa Florida

[2]Department of Cell Biology and Anatomy University of Arizona, Tucson AZ

[3]Internal Medicine, University of California Davis, Davis CA

[4]Immunolgy Program, Moffitt Cancer Center

[5]Drug Discovery Program Moffitt Cancer Center

[6]Experimental Therapeutics Program, Moffitt Cancer Center

Abstract

HYD1 is a D-amino acid peptide that was previously shown to inhibit adhesion of prostate cancer cells to the extracellular matrix. In this study, we show that in addition to inhibiting adhesion of multiple myeloma (MM) cells to fibronectin, HYD1 induces cell death in MM cells as a single agent. HYD1-induced cell death was necrotic in nature as shown by: (a) decrease in mitochondrial membrane potential ($\Delta\psi_m$); (b) loss of total cellular ATP, and; (c) increase in reactive oxygen species (ROS) production. Moreover, HYD1 treatment does not result in apoptotic cell death as it did not trigger the activation of caspases or the release of apoptosis-inducing factor (AIF) and Endonuclease G (Endo G) from the mitochondria, nor did it induce double stranded DNA breaks. HYD1 did initiate autophagy in cells; however, autophagy was found to be an adaptive response contributing to cell survival rather than the cause of cell death. We were further able to show that *N*-acetyl-L-cysteine (NAC), a thiol containing free radical scavenger, partially protects MM cells from HYD1-induced death. Additionally NAC blocked HYD1- induced as well as basal levels of autophagy, suggesting that ROS can potentially trigger both cell death and cell survival pathways. Taken together, our data describe an important role of ROS in HYD1-induced necrotic cell death in MM cells.

Introduction

Despite recent advances in the treatment of multiple myeloma (MM), the disease remains incurable. There is accumulating evidence that targeting multiple cell death pathways may be an advantageous strategy for treating cancers such as MM, which are currently not cured by standard therapy that targets the apoptotic pathway (for review see, (1)). Cell death in mammalian cells can be broadly classified into three types. Morphologically, type I cell death (apoptosis) is characterized by chromatin condensation and DNA fragmentation; type II cell death (autophagy) is characterized by a massive accumulation of double-membraned vesicles commonly referred to as autophagosomes, and type III cell death (necrosis) is characterized by oncosis and plasma membrane rupture (2). Although all three types have been shown to

To whom correspondence should be addressed as follows: Dr. Lori Hazlehurst, Molecular Oncology, H Lee Moffitt Cancer Center Tampa, FL, USA., Phone: 813-903-6807, Fax: 813-979-7265, Email: Lori.Hazlehurst@moffitt.org.
*contributed equally to the manuscript.

undergo a sequential programmed cell death (PCD) mechanism, the majority of conventional anti-cancer therapeutic agents used in hematologic malignancies utilize the apoptotic pathway to induce cell death (for review see, (3)). Unfortunately, during progression towards drug resistant disease the apoptotic machinery, consisting of anti-apoptotic and pro-apoptotic proteins, is not balanced and often favors cell survival following cytotoxic insult. In such a scenario, agents that initiate non-apoptotic cell death may easily overcome the inherent deficiencies of the apoptotic machinery in cancer cells. As a result targeting alternative cell death pathways may represent an attractive approach to increasing overall tumor cell kill.

Necrosis is often defined as a default cell death pathway. This concept is supported by evidence that in mouse embryonic fibroblasts and in immortalized baby mouse kidney epithelial cells, over expressing anti-apoptotic protein Bcl-2, or simultaneous knockdown of pro-apoptotic proteins Bax or Bak (apoptotic pathway) and depletion of beclin-1 (autophagic pathway), leads to necrotic cell death when exposed to hypoxia or etoposide (4,5). In terms of biochemical changes, loss of $\Delta\psi_m$ is considered a hallmark feature of necrotic cell death. $\Delta\psi_m$ loss has been attributed to be a response to a rise in cytosolic free calcium, anoxia and overproduction of reactive oxygen species (ROS) (for review see, 6). Although both apoptosis and necrosis require $\Delta\psi_m$ loss, the distinguishing difference between the two is that in necrosis $\Delta\psi_m$ loss is accompanied by a total cellular loss in ATP, which is maintained and required for apoptosis (7).

In the present study we show that HYD1 (kikmviswkg) a 10 D-amino acid containing peptide previously reported to block cell adhesion to the matrix in epithelial prostate carcinoma cells (8), can induce cell death in H929, 8226 and U266 MM cell lines but not in CD34+ hematopoietic progenitor cells or peripheral blood mononuclear cells (PBMC). The induction of cell death is distinct from apoptosis and autophagy, and is associated with the loss of $\Delta\psi_m$, ATP depletion and the induction of ROS. Furthermore, HYD1-induced necrotic cell death was partially reversible by pretreatment with NAC. Paradoxically, increased ROS in HYD1 treated cells results in the induction of autophagy, which protects cells against HYD1-induced necrotic cell death. In summary, these data provides rationale for further pre-clinical development of HYD1 and HYD1 derivatives that preferentially target alternative cell death pathways.

Materials and Methods

Cell culture

H929, 8226 and U266 cells were obtained from the American Type Culture Collection (Rockville, MD) and maintained at 37°C in 5% CO_2/95% air atmosphere. Cells were grown in suspension in RPMI 1640 media (Cellgro, Fischer Scientific Pittsburgh, PA), supplemented with fetal bovine serum (Omega Scientific, Turzana CA) (10% in H929 and U266 cell and 5% in 8226 cells), penicillin (100 ug/ml), streptomycin (100 ug/ml) and 2 mM L-glutamine (GIBCO-BRL, Grand Island, NY). For H929 cells 0.05 mM 2-mercaptoethanol was added to the culture media.

Chemical reagents, antibodies and peptides

5-(and-6)-carboxy-2',7' – dichlorodihydrofluorescein diacetate (carboxy-H_2DCFDA), 5-chloromethylfluorescein diacetate (CMFDA) and 3,3'-dihexyloxacarbocyanine iodide ($DiOC_6(3)$) were purchased from Invitrogen (Carlsbad, CA). Tunicamycin, Melphalan, *N*-acetyl-L-cystein (NAC), *tert*-butyl hydroperoxide (TBHP), melphalan and 3-Methyladenine (3-MA) were purchased from Sigma Aldrich (St.Louis, MO). Recombinant soluble *Killer*TRAIL was purchased from Alexis Biochemicals (San Diego,CA). z-VAD-fmk, pan caspase inhibitor was purchased from BD Biosciences (San Jose, CA). The anti- α4 integrin

(clone P4G9) was purchased from Abcam (Cambridge MA), anti- α5 integrin (clone P1D6) was purchased from Calbiochem (Gibbstown, NJ) and the anti-β1 integrin (AIIB2) was a generous gift of Dr. Anne Cress; anti-topoisomerase II β from BD Biosciences (San Jose, CA); anti-Bax (N20) was purchased from Santa Cruz Biotechnologies (Santa Cruz, CA); anti-LC-3 and anti-EndoG from Novus Biologicals (Littleton, CO), anti-β-actin, anti-Bax (6A7) and anti-α-tubulin from Sigma Aldrich (St.Louis, MO). Anti-caspase-8, caspase-9, caspase-3, anti-Beclin1 and anti-AIF were purchased from Cell Signaling (Danvers, MA). HYD1 (kikmviswkg) and HYDS (wiksmkivkg) D-amino acid peptides were synthesized by Global Peptides (Fort Collins, CO).

Quantification of cell adhesion to fibronectin

Briefly, H929 myeloma cells were pre-incubated with varying concentrations of either HYD1 or the scrambled peptide (HYDS) for 30 minutes prior to allowing cells to attach to FN for two hours. Cell adhesion was detected by crystal violet staining as previously described (9,10).

Quantification of cell adhesion to HS-5 bone marrow stroma cells

Adhesion of H929 cells to the HS-5 bone marrow stroma cell line was performed as previously described (11).

Co-culture model of drug resistance

HS-5 ectopically expressing GFP were plated at a density of 200,000 cells per ml overnight in a 6 well plate. The following day H929 cells at a density of 200,000 cells were incubated for 30 minutes with either 50 ug/ml HYDS, HYD1 or vehicle control (ddH20) and then added to HS-5 cells. H929 cells were allowed to adhere for 3 hrs prior to the addition of 15 uM melphalan to appropriate samples. Cell death was measured 24 hours later using annexin V-PE staining. Positive GFP expressing events were gated out of the analysis.

Cell death analysis

Cells were washed with an annexin binding buffer (BioVision Inc., Mountain View, CA) and incubated with either Annexin V-PE or a combination of Annexin V-FITC/PI. The cells were then analyzed for fluorescence using FACScan (BD Biosciences, San Jose, CA). Caspase 3 and 8 activity was measured at 6 and 24 hrs post peptide treatment per manufacturer's instructions (BD Biosciences, San Jose, CA).

Clonogenic assay

H929 cells were treated with HYD1 for 2 hrs and then diluted to 0.3% final agar solution reconstituted in growth media and then dispersed in triplicate in 35 mm culture plates containing 2,500 cells in each plate. Once the agar solidifies, cells were allowed to incubate for 12 additional days. Cell colonies (>50 cells) were then counted on 2 mm grid culture dish (Corning).

Colony formation assay

Whole blood from healthy donors was used to isolate CD34+ hematopoeitic progenitor cells with the aid of a CD34 MicroBead kit (Miltenyi Biotec Inc., Auburn, CA). The CD34+ cells were then washed and resuspended in Incomplete MethoCult Media supplemented with 2% FBS and treated for 2 hrs with HYD1 (StemCell Technologies, Vancouver, BC). The cells were then diluted in MethoCult (StemCell Technologies, Vancouver, BC) and then dispensed in duplicate 35 mm culture plates, containing 5000 cells in each plate. Colonies were scored on day 12.

Immunoprecipitation

After treatment, cells were lysed and 500 μg of cell lysate was incubated overnight with anti-Bax (6A7) at 4°C. Following incubation, lysates where further incubated with 25 μl of A/G beads for 2 hrs. The lysate mixture was then washed thrice with CHAPS lysis buffer and the immunoprecipitated proteins were then subjected to western blotting as described below. Anti-Bax (N20) antibody was used to probe for Bax protein.

Neutral Comet Assay

Cells were treated with either 50 ug/ml HYD1, HYDS or 50 ng/ml TRAIL for 6 hours. Following drug treatment 5,000 cells were pelleted and resuspendend in PBS agar solution and overlayed onto fully frosted glass slides. The neutral comet assay was performed as previously described by our laboratory (12).

Western blotting

Cells were plated in a 6-well plate at a concentration of 400,000 cells/ml. After treatment, cells were placed on ice and lysed in 100 μl of cold lysis buffer (120 mM NaCL, 50 mM Tris HCL pH 7.6, 0.5% NP-40, 1 mM EDTA, 1mM Na_3VO_4, 1 mM PMSF, and 1 μg/ml aprotinin and leupeptin). 10 μg of total protein was applied to an 8% SDS-PAGE gel. Proteins were resolved by electrophoresis and then transferred to a polyvinylidene fluoride (PVDF) membrane.

Electron Microscopy

H929 cells were treated for four hours with either 50 μg/ml HYD1 or HYDS for four hours. After peptide treatment, samples were fixed overnight in 2.5% glutaraldehyde in 0.1M phosphate buffer pH 7.2 at four degrees. Following fixation and dehydration with acetone, samples were suspended in 1:1 mixture of 100% acetone:embedding medium for 1 hour while under vacuum. Thin sections (80–90nm) were picked up on 100 mesh copper grids, stained with 8% aqueous uranyl acetate for 10 minutes, and Reynold's lead citrate for 5 minutes. Thin sections were examined with a Philips CM10 transmission electron microscope at 60kV. Representative cells were photographed, printed and scanned.

siRNA transfection

Transfection of H929 cells was performed as previously described (13). Briefly, 3.5 million H929 cells were added to 200 μl of cytomix buffer at pH 7.6 containing 120 mM KCl, 0.15 mM $CaCl_2$, 10 mM K_2HPO_4/KH_2PO_4, 25 mM Hepes, 2 mM EGTA, 5 mM $MgCl_2$, 2 mM ATP, 5 mM glutathione and 1.25 % DMSO. 10 μl of a 20 μM stock siRNA directed at Beclin1 (Dharmacon Lafayette, CO) or non silencing (Dhramacon) was added to the buffer. The mixture was placed in a 2 mm cuvette and electroporation was done at 140V/975 μF. After transfection, cells were incubated in the buffer for 15 minutes at 37°C. The mixture was transferred to a 25 ml flask containing 10 ml of fresh media. Cells were incubated for an additional 72 hours before treatment with HYD1.

Measurement of reactive oxygen species

Cells were suspended in pre-warmed PBS containing 5 μM of carboxy-H_2DCFDA for 20 min. The cells were then washed to remove the unloaded dye, returned to pre-warmed growth media and further incubated for 30 min. During the recovery period, where indicated, cells were treated with NAC (10 mM). The cells were treated as indicated and the fluorescence intensity was analyzed using Wallace VICTOR^2 1420 multilabel counter (EG&G Wallac, Turku, Finland) (excitation: 485 nm, emission: 535 nm).

Measurement of mitochondrial membrane potential ($\Delta\psi_m$)

After treatment, cells were incubated for 15 min with 15 nM of $DiOC_6$ (Molecular Probes Invitrogen). Cells were washed with PBS and resuspended in 500 μl of PBS and the loss of $\Delta\psi_m$ in cells was then analyzed using FACScan (BD Biosciences, San Jose, CA)

ATP measurement

Treated cells were lysed in RIPA lysis buffer (Upstate, Lake Placid, NY) and ATP concentrations were measured using ENLITEN ATP assay system bioluminescence detection kit as per manufacturer's instruction (Promega, Madison, WI). The ATP concentration was later normalized to the protein content of the lysates.

SCID-Hu model

The SCID-Hu model was performed as previously described (14). Briefly, SCID/Beige mice 4–6 weeks old were purchased from Taconic (Germantown, NY). Fetal tissue (18–23 weeks) was obtained from Advance Bioscience Resource (Alameda, CA) in compliance with state and federal government regulations. Two bones were surgically implanted in the mammary fat pad of 6–8 week female SCID mice. Following six weeks of bone engraftment 50,000 H929 cells were injected directly into the bone and tumor was allowed to engraft for 4 weeks. At 28 days, baseline tumor burden was quantified in the sera using a kappa ELISA kit per manufacture instructions (Bethyl, Montgomery, TX) and mice were randomized into treatment groups. HYD1 mice were treated with 8 mg/kg, (i.p.) daily as indicated for 21 days. Tumor burden was assessed weekly by measuring kappa levels in the sera.

Statistical analysis

Experiments were independently performed three times, unless specified otherwise in the legend. The data was plotted as mean ± SD, and analyzed for statistical significance between treatment groups using ANOVA followed by *post hoc*, Student's-Newman Keuls test. For dose response curves depicted in Figure 4C and 5B a paired t-test was used as the test for comparisons between treatment groups. For the *in vivo* study, the data was plotted as mean ± SD and analyzed for statistical significance using repeated measures ANOVA. A $P < 0.05$ was accepted as statistically significant.

Results

HYD-1 blocks adhesion to FN, induces cell death in MM cells *in vitro* and reverses resistance associated with the bone marrow stroma co-culture model

HYD1 was previously shown to inhibit integrin dependent cell adhesion in epithelial prostate carcinoma (8,15). Similarly, in this study we show that HYD1 blocks α4β1 mediated adhesion of MM cells to fibronectin (see Figure 1A). In contrast, HYD1 did not block MM cell adhesion to bone marrow stroma cells, a finding that was consistent with a β1 blocking antibody (see Figure 1B), suggesting that multiple cell adhesion molecules regulate adhesion of MM cells to bone marrow stroma. We postulated that if β1 integrin and not cell attachment were important in conferring drug resistance, then HYD1 treatment should reverse resistance associated with the co-culture model. As shown in Figure 1C, HYD1 treatment reduced the level of resistance to melphalan in the bone marrow stroma co-culture model system a finding that was more dramatic in 8226 cells compared to H929 cells (see figure 1C and S1). Upon testing HYD1 in the co-culture model system, an unanticipated observation was that HYD1 treatment induced cell death in suspension cultures as a single agent. Furthermore, MM cells were not resistant to HYD1 in the context of the co-culture model (see Figure 1D). Finally, HYD1 increased the levels of melphalan specific cell death in both suspension and co-culture conditions.

Due to the finding that HYD1 induced equivalent cell death in MM cells as a single agent in both suspension cultures and in the co-culture model we decided to further investigate the mechanism of action of HYD1 induced cell death in suspension cultures. MM cells were treated with 12.5 or 50 ug/ml of HYD1, or the scrambled peptide control HYDS, for 6 hours followed by measurement of annexin V positive cells, used as a marker for cell death. As shown in figure 2A, HYD1 treatment increased annexin V positive cell staining compared to cells treated with the scrambled variant HYDS in H929 cells. Additionally, as shown in figure 2B, HYD1 inhibited in a dose dependent manner the ability of H929 cells to form colonies in soft agar. HYD1 was also found to induce cell death in 8226 and U226 cells (see figure 2C and 2D).

HYD1 does not induce apoptotic cell death

In order to examine if HYD1-induced cell death was dependent on the apoptotic pathway involving caspases, we investigated the processing and activation of caspases. As seen in figure 3A, 6 hours treatment with 50 μg/ml of HYD1 did not result in the activation of caspase-8 and only a minimal activation of caspase-3. Also, HYD1 treatment did not give rise to cleaved active form of caspase−3, −9 and −8 as ascertained by western blot analysis in H929 cells (figure 3B). The absence of cleaved caspases was also observed in 8226 cells (supplementary data S2). Endonuclease G (Endo G) and apoptosis inducing factor (AIF), depending on the cellular context and cytotoxic insult have been reported to be released from the mitochondria in both a caspase dependent and independent manner (16, 17). Proapoptotic protein Bax has been implicated in the formation of outer membrane mitochondrial pore, causing the release of AIF and Endo G from the mitochondria. This is followed by translocation of AIF and Endo G to the nucleus, leading to DNA fragmentation and nuclear condensation (18). To first investigate whether HYD1 caused a conformational change in Bax, we performed immunoprecipitation in order to pull down the active form of Bax (19). As shown in figure 3C, HYD1 treatment failed to increase the proportion of active Bax, as the levels were comparable to those seen in HYDS treated and control cells. We followed this study by performing a cellular enrichment of treated cells into the nuclear and the cytosolic fraction. As shown in figure 3C, no translocation of AIF or Endo G from the cytoplasm to the nucleus was observed after 6 hour treatment with HYD1. These data indicate that HYD1 treatment does not lead to cell death via a caspase independent translocation of Endo G and AIF from the mitochondria to the nucleus. Finally, double-stranded DNA breaks resulting from the internucleasomal DNA cleavage by endonucleases (mediated predominately by caspase activated DNAse, lysosomal DNAse II and Endo G) is an important biochemical marker for apoptotic cell death (20). To determine if double stranded breaks are involved in HYD1-induced cell death, H929 cells were treated for 6 hours with HYD1 and then subjected to neutral comet assay. TRAIL was used as a positive control for apoptotic cell death. As seen in figure 3D, TRAIL treatment lead to a significant increase in comet moments. However, HYD1, HYDS and control cells showed equivalent comet moments indicating the absence of activation of endonucleases and double stranded DNA breaks in HYD1 treated cells.

Finally we determined whether HYD1 induced a latent induction of caspases. The pan caspase inhibitor zVAD-fmk was used to determine whether caspases contributed to HYD1 induced cell death following 24 hours of HYD1 treatment. As shown in supplemental data S3, pretreatment of H929 cells with zVAD-fmk did not inhibit cell death induced by HYD1. In contrast, zVAD-fmk treatment blocked the majority of the melphalan-treated annexin V positive cells. Of note with HYD1 treatment, PI and annexin V positivity occur simultaneously, which is not the case for melphalan treatment in which you can observe a predominant annexin V positive and PI negative cell population. These data were consistent with caspase activity assays which demonstrated that neither caspase 3 or 8 activity was induced following 24 hours of HYD1 treatment (see supplemental data S3). Taken together, these data demonstrates that

HYD1-induced cell death occurs independent of caspase and endonuclease activity, indicating that HYD1 does not induce apoptosis in MM cells.

HYD1 induces autophagy in MM cells

We utilized electron microscopy to observe the morphology of HYD1 treated cells. As shown in figure 4A, 4 hours treatment with HYD1 in H929 cells revealed the presence of several autophagosomes, observed as extensive double-membrane vacuolar structure containing cytoplasmic contents. Such autophagosomes were absent in HYDS treated cells. Another hallmark of autophagy is the lipidation of LC3 protein, which can be detected by western blot analysis (21). Thus, we performed western blot analysis to determine whether HYD1 treatment caused the conversion of cytoplasmic form of LC3 (LC3-I, 18 k Da) to the autophagosomal membrane-bound form of LC3 (LC3-II, 16 k Da). As seen in figure 4A, and consistent with the electron microscopy data, a 4 hour treatment with HYD1 and tunicamycin, a known inducer of autophagy, resulted in increased conversion of LC3-I to LC3-II. Additional markers of autophagy include an increase in the formation of acidic vesicles. As shown in supplemental data S4, HYD1 treatment caused an increase in the number and size of acidic vesicles as shown by lysosensor staining.

Autophagy induced by HYD1 protects the cells against death

Depending on the context, the induction of autophagy has been shown to be associated with cell survival or cell death (22,23). To determine whether autophagy induced by HYD1 plays a role in cell survival or cell death, we blocked autophagy by two independent methods. We used siRNA targeting Beclin1, whose expression is required for the formation of pre-autophagosomal structures, and a pharmacological approach using 3-methyladenine (3-MA), a nucleotide derivative and class III PI-3 kinase inhibitor shown to inhibit the earliest stages of autophagosome formation (24,25). As seen in figure 4B & 4C, both strategies significantly sensitized H929 cells to HYD1-induced cell death. The addition of 3-MA also sensitized 8226 cells to HYD1 induced cell death (See supplemental data S5). These results indicate that autophagy is an adaptive response and contributes to survival of MM cells following HYD1 treatment. There is a mutual crosstalk between autophagy and apoptosis. It has been reported that certain stimuli can induce cells to undergo autophagic cell death, and upon inhibition of autophagy, under the same stimuli the cells revert to apoptotic cell death (26). To determine whether the increase in cell death observed upon HYD1 treatment under the inhibition of autophagy was due to a switch to apoptotic cell death, we pretreated cells with 3-MA followed by HYD1 and then looked for cleaved caspase−3, −8 and −9 in cell lysates by western blot analysis. As shown in Figure4D, neither 3-MA, HYD1 alone nor their combination caused cleavage of caspases. We further validated these findings by repeating the experiment in 8226 cells and found similar results (data not shown). Taken together these data indicate that inhibition of HYD1-induced autophagy does not sensitize MM cells to undergo caspase-dependent cell death.

HYD1 induced necrotic cell death

Major biochemical markers associated with necrotic cell death are the loss of $\Delta\psi_m$ accompanied by loss of total ATP and a rise in ROS production in cells. We found that HYD1 (50 ug/ml) treatment caused a significant loss of $\Delta\psi_m$ in H929 cells (see figure 5A). This was accompanied by a 62% decrease in ATP levels (see figure 5A). Additionally, HYD1 treatment resulted in a significant increase in ROS production when compared to control cells (see figure 5A). Similar results were found in 8226 cells (see supplementary data S6). All these events occurred rapidly during treatment with HYD1, suggesting that in MM cells HYD1 induces cell death through the necrotic cell death pathway.

ROS plays a role in the induction of cell death and autophagy in HYD1 treated MM cells

ROS has been shown to be an important mediator involved in propagation and execution of necrotic cell death. To investigate whether ROS is the cause of cell death in HYD1 treated cells, we pretreated cells with NAC, a thiol containing free radical scavenger. The dose of NAC used was shown to be effective in inhibiting the production of ROS (supplementary data S7). As seen in figure 5B, NAC partially protects H929 from HYD1 induced cell death. At the highest HYD1 concentration, NAC protected cells from death by 32% in H929 when compared to cells treated with HYD1 only. Similar results were found in U226 cells (see supplementary data S8). These data indicate that ROS plays an important role in inducing necrotic cell death in HYD1 treated MM cells.

Mitochondria are considered the major organelle capable of generating ROS within cells. In order to determine whether ROS was the cause or the product of loss of $\Delta\psi_m$, we pretreated cells with NAC and followed it by treatment with HYD1. As shown in figure 5C, the observed loss in $\Delta\psi_m$ was not reversed by pretreatment with NAC. These data suggest that ROS production lies downstream of disruption of $\Delta\psi_m$.

Finally, oxidative stress has been shown to induce autophagy (22). In order to investigate whether autophagy observed in HYD1-treated cells was due to the induction of ROS, we pretreated cells with NAC followed by HYD1 treatment. As shown in figure 5D, HYD1 caused a substantial increase in LC3-II formation when compared to control cells. The increase in LC3-II was completely reversed by pretreating cells with NAC. Moreover, the addition of NAC reversed basal levels of LC3-II, suggesting that autophagy is driven by endogenous ROS levels in MM cells and may be a general mechanism whereby cancer cells can tolerate high basal levels of ROS typically associated with transformation. Taken together, these data show that HYD1 induces ROS downstream of disruption of mitochondria membrane potential. Additionally HYD1 induction of ROS can paradoxically contribute to both cell survival by inducing autophagy and cell death by inducing necrosis in MM cells.

HYD1 demonstrates decreased potency in normal hematopoietic progenitor cells and retains modest *in vivo* activity

A colony forming assay was used to determine whether HYD1 induced cell death in normal hematopoietic cells. As shown in figure 6A, HYD1 did not inhibit colony formation of normal $CD34^+$ cells. In addition, we evaluated the toxicity of HYD1 in normal peripheral blood mononuclear cells (PBMC). As seen in figure 6B, six hours treatment with increasing concentration of HYD1 did not induce cell death up to doses of 50 μg/ml in PBMC. Together our data indicate that HYD1 targets MM cells preferentially when compared to normal hematopoietic cells

Finally, we used the SCID-hu model to determine whether HYD1 demonstrates anti-tumor activity *in vivo*. The SCID-hu model consists of implanting human fetal bone into the mammary mouse fat pad of SCID mice. Circulating kappa levels were measured on day 28 (baseline reading before peptide treatment), 35, 42 and 49 by ELISA. Shown in figure 6C, is the antitumor response of H929 engrafted tumor when mice were given 8 mg/kg intraperitoneal (i.p.) injections daily for 21 days starting on day 28. Mice treated with HYD1 showed a modest but significant reduction in tumor burden compared to control mice. In these experiments no overt toxicity or weight loss was noted in HYD1 treated animals. Further studies are warranted to determine whether the *in vivo* activity of HYD1 can be improved by using PEGylation or cyclization strategies to increase the bioavailability and potentially the anti-tumor activity of HYD1. Represented in figure 6D is our working model of the mechanism of action associated with HYD1 induced cell death. Based on our results further studies are warranted to determine

the upstream targets causative for HYD1 induced depolarization of the mitochondria membrane potential.

Discussion

HYD1 was previously identified using a combinatorial peptide synthesis in combination with an adhesion based screen (15). HYD1 has been previously shown to block random haptotactic migration and inhibit invasion of epithelial prostate carcinoma cells on laminin-5 (laminin 332) (8). These studies demonstrated that HYD1 interacted with α6 and α3 integrin (laminin receptors) on the tumor cell surface and blocked adhesion while inducing an elevation of laminin-5 (laminin 332)-dependent intracellular signaling, including focal adhesion kinase, mitogen-activated protein kinase kinase and extracellular signal-regulated kinase (8). Currently it is unclear if cell death associated with HYD1 treatment is due to direct binding of the α subunit or whether HYD1 interacts with an integrin binding death inducing partner, associated with a specific α subunits, in a multi-protein complex. It must be noted that a β1 blocking antibody does not induce cell death in MM cells (data not shown) indicating that HYD1 has unique binding properties and may indeed act as an agonist for inducing cell death. Further studies are warranted to validate HYD1 target(s) associated with the induction of cell death.

In addition to blocking cell adhesion and reversing resistance associated with the HS-5 bone marrow stroma co-culture model, we have demonstrated in this report for the first time that HYD1, a D-amino acid peptide, induces cell death as a single agent in MM cells grown *in vitro*. More importantly, HYD1 treatment was found to be less-toxic to $CD34^+$ progenitor cells and PBMC compared to MM cells. We further show that HYD1-induced cell death in MM cells demonstrated markers that are characteristic of necrosis, as cell death was accompanied by loss of $\Delta\psi_m$, decrease in total cellular ATP and a significant increase in ROS. Also, HYD1-induced cell death could be partially reversed by pre-treating cells with the ROS scavenger, NAC. Another interesting finding in our study is that the oxidative stress induced by HYD1 resulted in the initiation of an autophagic pathway which paradoxically protected the cells against HYD1-induced cell death.

Caspase-dependent apoptosis is induced through two major pathways; one involves the death receptor, called the extrinsic pathway, and utilizes caspase-8 and another is the intrinsic pathway, involving the mitochondria and mediated by caspase-9 (27,28). Both of these pathways converge on caspase-3 activation, eventually resulting in DNA fragmentation (29). In our study HYD1 did not activate either the intrinsic or the extrinsic pathway of apoptosis as confirmed by measuring three different end points; (a) absence of cleaved caspases in HYD1 treated cells by western blotting, (b) absence of caspase activity in HYD1 treated cells by substrate cleavage and (c) failure of zVAD-fmk, a pan caspase inhibitor to block HYD1-induced cell death as ascertained by annexin v-FITC/PI binding studies.

DNA fragmentation can also occur through the mitochondrial death effector proteins AIF and Endo G. Under some cytotoxic stimuli, both AIF and Endo G are released from the mitochondria and translocate to the nucleus where they cause large scale DNA fragmentation (29,30). In our study, HYD1 did not trigger the translocation of AIF and Endo G to the nucleus. This observation was consistent with the finding that HYD1 treatment did not activate Bax or caspases. Importantly these studies were performed in cell lines capable of activating caspases. Thus in the cell lines tested, HYD1 activates caspase independent cell death not as a default pathway but rather as a primary mode of cell death.

Necrosis is the consequence of extensive crosstalk between several biochemical and molecular events. Currently there is no single well-described signaling cascade to define necrotic cell death (for review see, (31)). Similarly in our study, we show three different biochemical events,

namely loss of $\Delta\psi_m$, decrease in cellular ATP and increased production of ROS as evidence for the HYD1-induced necrotic cell death. Further studies are warranted to determine the mechanism of HYD1 induced loss of $\Delta\psi_m$ without activation of Bax, release of AIF and Endo-G or activation of capsases. Likely candidates for the cause of HYD1-induced loss of $\Delta\psi_m$ may include activated Bcl-2 family member BNIP3, cyclophilin D or calcium overload, all of which either alone or in concert are reported to cause a decrease in mitochondrial membrane potential without release of intermembrane space proteins (6,32,33). Loss of $\Delta\psi_m$ can lead to mitochondrial dysfunction resulting in a breakdown of the respiratory chain and the overproduction of ROS concomitant with uncontrolled hydrolysis of ATP, ultimately leading to necrotic cell death (34). Interestingly, in our study ROS seems to be a major player in the induction of necrotic cell death, as we could partially reverse HYD1-induced cell death by pre-treating the cells with a ROS scavenger, NAC.

In the present study, in addition to necrotic cell death, we show that HYD1 treatment resulted in a manifestation of morphological and biochemical markers that are indicative of autophagy. These markers included the extensive formation of double membrane containing vesicles and lipidation of LC3. Even though autophagy is a ubiquitous process in mammalian cells that contributes to the routine turnover of cytoplasmic components in case of cellular stress, autophagy can act as a defense mechanism involving the removal and recycling of damaged proteins and organelles by delivering them to lysosomes (for review see, (35)). In the present study we show that an increase in ROS, in HYD1 treated cells results in the induction of autophagy. This observation is consistent with previous reports showing the elevated ROS levels-induces autophagy via the oxidation of a cysteine residue on Atg4 (36).

In summary, these studies show that while HYD1 can block α4β1 integrin dependent binding of MM cells to FN, HYD1 also induces cell death *in vitro*. Although the *in vivo* activity was modest, we are currently pursuing strategies such as PEGylation and cyclization which will increase the bioavailability of the peptide *in vivo*. Importantly HYD1 increased the levels of melphalan specific cell death and reversed resistance to melphalan associated cell death when co-culturing myeloma cells with the bone marrow stroma cell line HS-5. Together these data suggest that HYD1 may be an attractive agent to combine with agents that a) target the apoptotic machinery and b) are resistant in a bone marrow stroma co-culture model system. Mechanistically HYD1 treatment leads to the loss of $\Delta\psi_m$ and a decrease in cellular ATP resulting in an increase in ROS production. All of these three biochemical events ultimately lead to a necrotic cell death in MM cells. Moreover, we anticipate that HYD1 will prove to be an important tool to dissect the molecular pathway of caspase independent cell death and allow for investigations for deciphering crosstalk between apoptotic and non-apoptotic cell death pathways. Finally, drug resistance is often associated with an imbalance in pro and anti-apoptotic mediators with the net result favoring cell survival. Thus, agents such as HYD1 that preferentially target alternative cell death pathways may provide an ideal strategy for developing combination therapies to eliminate sub-population of cells resistant to apoptotic cell death.

Supplementary Material

Refer to Web version on PubMed Central for supplementary material.

Acknowledgments

This work was supported by National Cancer Institute R01CA122065 (LAH) and by the Multiple Myeloma Research Foundation (LAH)

References

1. Hu X, Xuan Y. Bypassing cancer drug resistance by activating multiple death pathways-a proposal from the study of circumventing cancer drug resistance by induction of necroptosis. Cancer Lett 2008;259:127–137. [PubMed: 18082322]
2. Galluzzi L, Maiuri MC, Vitale I, et al. Cell death modalities: classification and pathophysiological implications. Cell Death Differ 2007;14:1237–1243. [PubMed: 17431418]
3. Reed JC, Pellecchia M. Apoptosis-based therapies for hematologic malignancies. Blood 2005;106:408–418. [PubMed: 15797997]
4. Degenhardt K, Mathew R, Beaudoin B, et al. Autophagy promotes tumor cell survival and restricts necrosis, inflammation, and tumorigenesis. Cancer cell 2006;10:51–64. [PubMed: 16843265]
5. Shimizu S, Kanaseki T, Mizushima N, et al. Role of Bcl-2 family proteins in a non-apoptotic programmed cell death dependent on autophagy genes. Nat Cell Biol 2004;6:1221–1228. [PubMed: 15558033]
6. Brookes PS, Yoon Y, Robotham JL, Anders MW, Sheu SS. Calcium, ATP, and ROS: a mitochondrial love-hate triangle. Am J Physiol 2004;287:C817–C833.
7. Leist M, Single B, Castoldi AF, Kuhnle S, Nicotera P. Intracellular adenosine triphosphate (ATP) concentration: a switch in the decision between apoptosis and necrosis. J Exp Med 1997;185:1481–1486. [PubMed: 9126928]
8. Sroka TC, Pennington ME, Cress AE. Synthetic D-amino acid peptide inhibits tumor cell motility on laminin-5. Carcinogenesis 2006;27:1748–1757. [PubMed: 16537560]
9. Damiano JS, Cress AE, Hazlehurst LA, Shtil AA, Dalton WS. Cell adhesion mediated drug resistance (CAM-DR): role of integrins and resistance to apoptosis in human myeloma cell lines. Blood 1999;93:1658–1667. [PubMed: 10029595]
10. Hazlehurst LA, Damiano JS, Buyuksal I, Pledger WJ, Dalton WS. Adhesion to fibronectin via beta1 integrins regulates p27kip1 levels and contributes to cell adhesion mediated drug resistance (CAM-DR). Oncogene 2000;19:4319–4327. [PubMed: 10980607]
11. Nefedova Y, Landowski TH, Dalton WS. Bone marrow stromal-derived soluble factors and direct cell contact contribute to de novo drug resistance of myeloma cells by distinct mechanisms. Leukemia 2003;17:1175–1182. [PubMed: 12764386]
12. Hazlehurst LA, Valkov N, Wisner L, et al. Reduction in drug-induced DNA double-strand breaks associated with beta1 integrin-mediated adhesion correlates with drug resistance in U937 cells. Blood 2001;98:1897–1903. [PubMed: 11535527]
13. Turner JG, Engel R, Derderian JA, Jove R, Sullivan DM. Human topoisomerase IIalpha nuclear export is mediated by two CRM-1-dependent nuclear export signals. J Cell Sci 2004;117:3061–3071. [PubMed: 15173319]
14. Zhu K, Gerbino E, Beaupre DM, et al. Farnesyltransferase inhibitor R115777 (Zarnestra, Tipifarnib) synergizes with paclitaxel to induce apoptosis and mitotic arrest and to inhibit tumor growth of multiple myeloma cells. Blood 2005;105:4759–4766. [PubMed: 15728126]
15. DeRoock IB, Pennington ME, Sroka TC, et al. Synthetic peptides inhibit adhesion of human tumor cells to extracellular matrix proteins. Cancer Res 2001;61:3308–3315. [PubMed: 11309285]
16. Arnoult D, Gaume B, Karbowski M, Sharpe JC, Cecconi F, Youle RJ. Mitochondrial release of AIF and EndoG requires caspase activation downstream of Bax/Bak-mediated permeabilization. EMBO J 2003;22:4385–4399. [PubMed: 12941691]
17. van Loo G, Schotte P, van Gurp M, et al. Endonuclease G: a mitochondrial protein released in apoptosis and involved in caspase-independent DNA degradation. Cell Death Differ 2001;8:1136–1142. [PubMed: 11753562]
18. Wang X, Yang C, Chai J, Shi Y, Xue D. Mechanisms of AIF-mediated apoptotic DNA degradation in Caenorhabditis elegans. Science 2002;298:1587–1592. [PubMed: 12446902]
19. Hsu YT, Youle RJ. Nonionic detergents induce dimerization among members of the Bcl-2 family. J Biol Chem 1997;272:13829–13834. [PubMed: 9153240]
20. Enari M, Sakahira H, Yokoyama H, Okawa K, Iwamatsu A, Nagata S. A caspase-activated DNase that degrades DNA during apoptosis, and its inhibitor ICAD. Nature 1998;391:43–50. [PubMed: 9422506]

21. Mizushima N, Yoshimori T. How to interpret LC3 immunoblotting. Autophagy 2007;3:542–545. [PubMed: 17611390]
22. Chen Y, McMillan-Ward E, Kong J, Israels SJ, Gibson SB. Oxidative stress induces autophagic cell death independent of apoptosis in transformed and cancer cells. Cell Death Differ 2008;15:171–182. [PubMed: 17917680]
23. Ogata M, Hino S, Saito A, et al. Autophagy is activated for cell survival after endoplasmic reticulum stress. Mol Cell Biol 2006;26:9220–9231. [PubMed: 17030611]
24. Mizushima N, Yamamoto A, Hatano M, et al. Dissection of autophagosome formation using Apg5-deficient mouse embryonic stem cells. J Cell Biol 2001;152:657–668. [PubMed: 11266458]
25. Seglen PO, Gordon PB. 3-Methyladenine: specific inhibitor of autophagic/lysosomal protein degradation in isolated rat hepatocytes. Proc Natl Acad Sci U S A 1982;79:1889–1892. [PubMed: 6952238]
26. Boya P, Gonzalez-Polo RA, Casares N, et al. Inhibition of macroautophagy triggers apoptosis. Mol Cell Biol 2005;25:1025–1040. [PubMed: 15657430]
27. Li H, Zhu H, Xu CJ, Yuan J. Cleavage of BID by caspase 8 mediates the mitochondrial damage in the Fas pathway of apoptosis. Cell 1998;94:491–501. [PubMed: 9727492]
28. Li P, Nijhawan D, Budihardjo I, et al. Cytochrome c and dATP-dependent formation of Apaf-1/caspase-9 complex initiates an apoptotic protease cascade. Cell 1997;91:479–489. [PubMed: 9390557]
29. Liu X, Zou H, Slaughter C, Wang X. a heterodimeric protein that functions downstream of caspase-3 to trigger DNA fragmentation during apoptosis. Cell 1997;89:175–184. [PubMed: 9108473]
30. Susin SA, Lorenzo HK, Zamzami N, et al. Molecular characterization of mitochondrial apoptosis-inducing factor. Nature 1999;397:441–446. [PubMed: 9989411]
31. Festjens N, Vanden Berghe T, Vandenabeele P. Necrosis, a well-orchestrated form of cell demise: signalling cascades, important mediators and concomitant immune response. Biochim Biophys Acta 2006;1757:1371–1387. [PubMed: 16950166]
32. Nakagawa T, Shimizu S, Watanabe T, et al. Cyclophilin D-dependent mitochondrial permeability transition regulates some necrotic but not apoptotic cell death. Nature 2005;434:652–658. [PubMed: 15800626]
33. Vande Velde C, Cizeau J, Dubik D, et al. BNIP3 and genetic control of necrosis-like cell death through the mitochondrial permeability transition pore. Mol Cell Biol 2000;20:5454–5468. [PubMed: 10891486]
34. Lemasters JJ, Nieminen AL, Qian T, et al. The mitochondrial permeability transition in cell death: a common mechanism in necrosis, apoptosis and autophagy. Biochim Biophys Acta 1998;1366:177–196. [PubMed: 9714796]
35. Klionsky DJ. Autophagy: from phenomenology to molecular understanding in less than a decade. Nat Rev 2007;9:931–937.
36. Scherz-Shouval R, Shvets E, Fass E, Shorer H, Gil L, Elazar Z. Reactive oxygen species are essential for autophagy and specifically regulate the activity of Atg4. EMBO J 2007;26:1749–1760. [PubMed: 17347651]

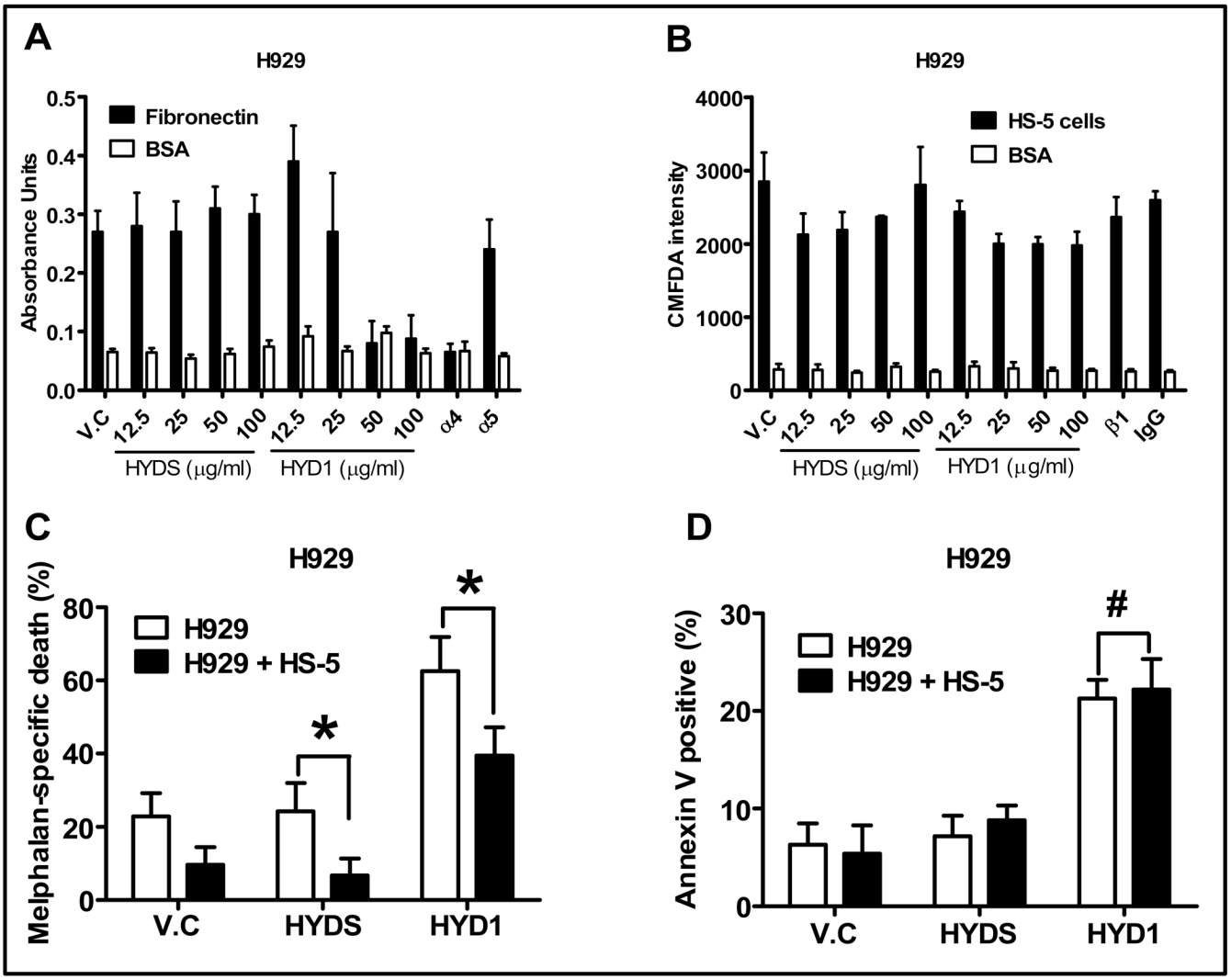

Figure 1. HYD1 blocks α4β1 mediated cell adhesion and induces equivalent cell death in suspension and in the HS-5 bone marrow stroma co-culture model

(A) H929 cells were pretreated for 30 minutes with varying doses of HYD1 or 1:100 dilution of α4 or α5 blocking antibody as described in materials and methods. Shown is a representative of three independent experiments performed in quadruplicate. (B) H929 cells were loaded with CMFDA as described in materials and methods and cells were pre-treated with the varying concentrations of HYD1 or a 1:100 dilution of β1 blocking antibody. Shown is a representative of three independent experiments performed in quadruplicate. (C) Co-culture model of drug resistance was studied in H929 cells as described in materials and methods. Melphalan specific cell death was calculated by subtracting out baseline death observed in control, HYD1 treated and HYDS treated cells. Thus HYD1 melphalan specific death equals % annexin V positive melphalan + HYD1 treatment- % annexin V positive in HYD1 treatment only. HYDS melphalan specific death equals % annexin V positive Melphalan + HYDS treatment-% annexin positive HYDS (n=9; *, $P<0.05$). (D) H929 cells were pretreated for 30 minutes with 50 ug/ml HYD1 prior to either growth in suspension or as a co-culture. 24 hours after drug treatment annexin V staining and FACS analysis was used to detect dead MM cells (n=9; #, $P>0.05$).

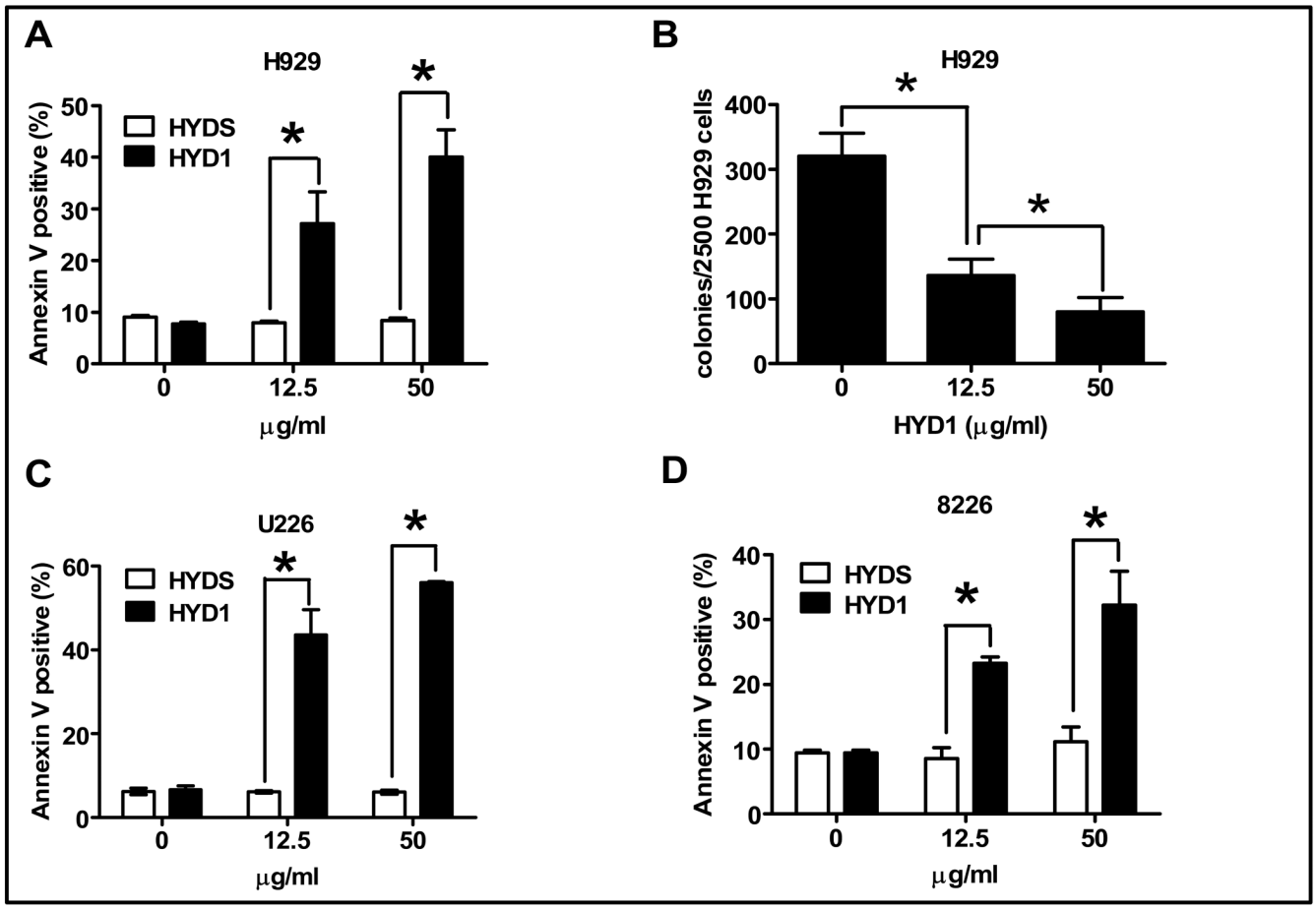

Figure 2. HYD1 induces cell death in MM cells

(A), (C) & (D) H929, U226 & 8226 cells, respectively were treated with either 0, 12.5 or 50 ug/ml HYD1 or HYDS for 6 hours. Annexin V positive cells were determined by FACS analysis. (B) 2,500 H929 cells were treated with HYD1 for 2 hours prior to being plated in triplicates in 0.3 % agar, supplemented with growth media. The numbers of colonies per 2,500 cells platted was counted after 12 days. Figures shown are a representative of three independent experiments performed in triplicate (n=9; *, $P<0.05$).

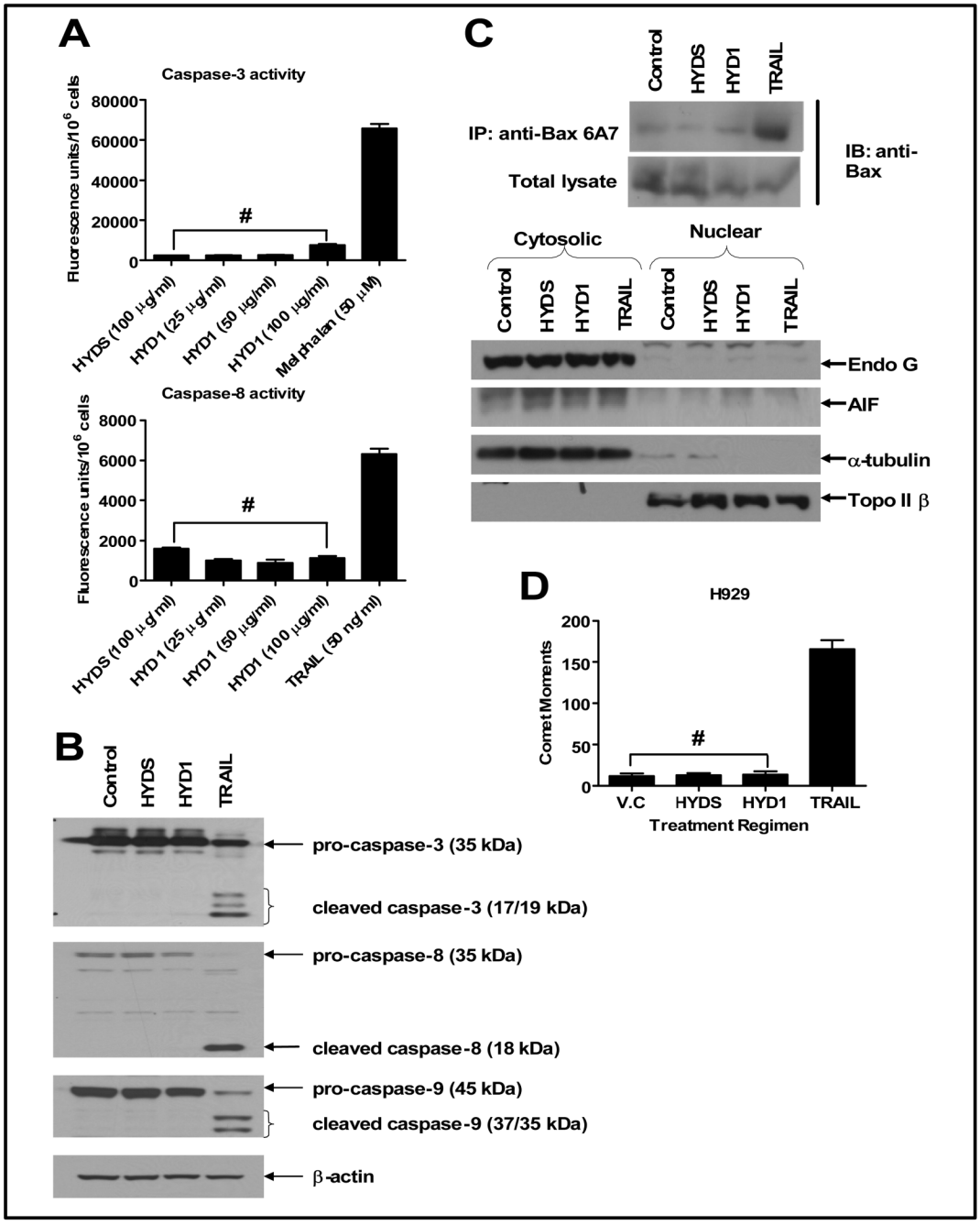

Figure 3. HYD1 does not induce apoptotic cell death in MM cells

(A) H929 (4×10^5 cells/ml) were plated in 24-well plates and treated with the indicated concentrations of either HYD1 or HYDS for 6 hrs followed by measurement of active caspase −3 and −8 as per manufacturers instruction (n=6; #, P>0.05). H929 cells (4×10^5 cells/ml) were treated for 6 hours with either 50 μg/ml of HYD1 and HYDS or 50 ng/ml of TRAIL. Following this, they were subjected to; (B) western blotting, probing for caspase−3, −8 and −9, (C) Immunoprecipitation, for active Bax using 6A7 antibody and then probed for Bax levels. Nuclear and cytoplasmic enriched extracts where probed for Endo G, AIF, α- tubulin and topoisomerase II β, and finally (D) neutral comet assay to measure double stranded DNA breaks. The comet moments were calculated by measuring 50 images for each treatment using

a CCD camera with Smart capture program (n=150; #, P>0.05). Figures shown are a representative of three independent experiments.

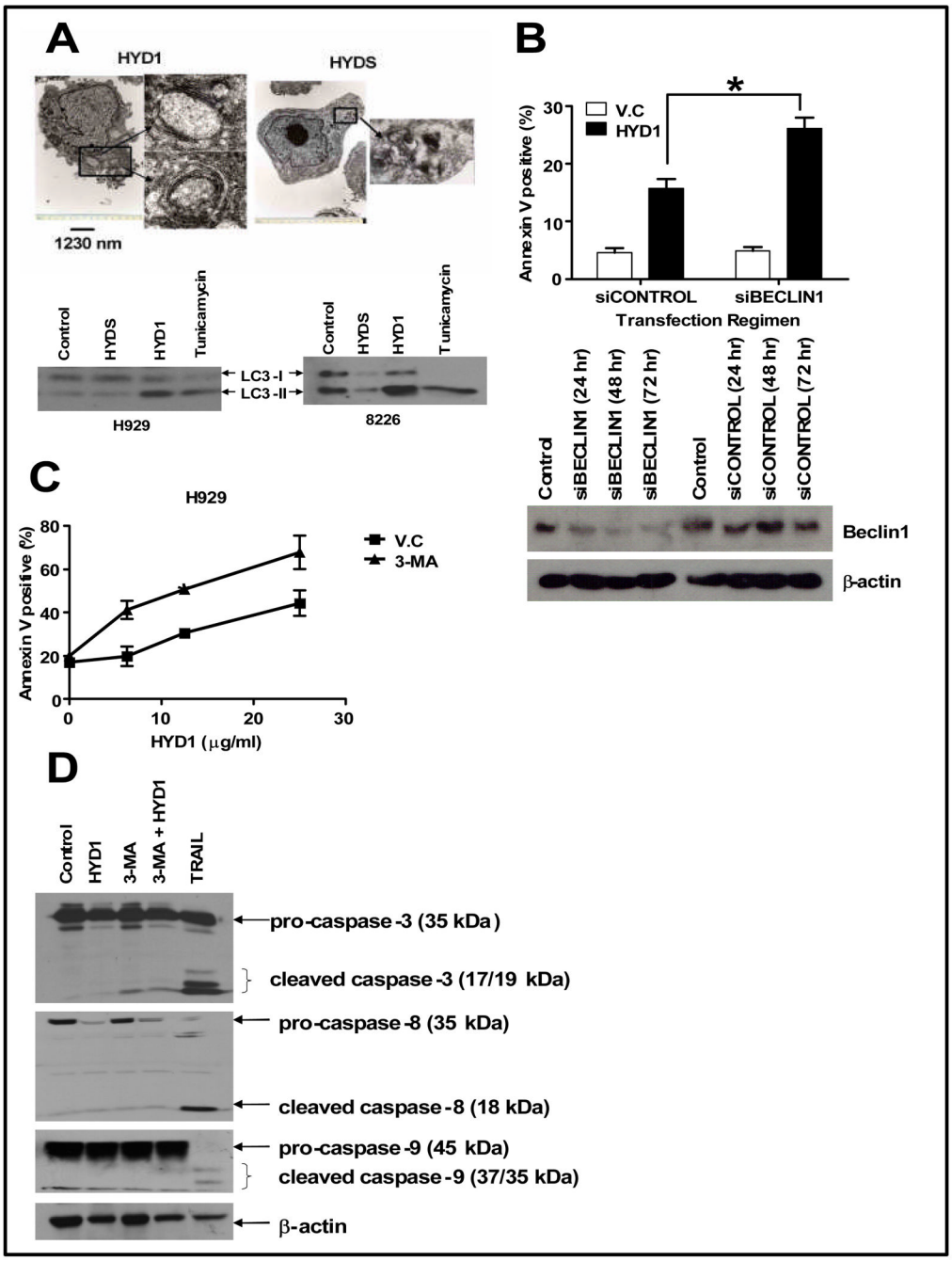

Figure 4. HYD1 induces autophagy which is cytoprotective in MM cells

(A) H929 cells were treated with either 50 ug/ml HYD1 or HYDS for 4 hrs and then processed for electron microscopy as described in the method section. H929 or 8226 cells were treated with either HYD1 or HYDS (50 μg/ml for H929 and 100 ug/ml for 8226 cells or 100 uM tunicaymcin for 4 hrs. Following treatment, LC3-1 to LC3-II conversion was monitored by western blot analysis. (B) H929 cells where transfected with a pool of 4 siRNA, targeting Beclin1 (siBECLIN1) or a control off Target siRNA (siCONTROL) using electroporation technique as described in materials and methods. 72 hrs post-transfection the cells where treated for 6 hrs with HYD1 (50 μg/ml) and cell death was determined by FACS analysis of annexin V positive cells (n=9; *, P<0.05). Also, (B) Western blot analysis showing the reduction of

Beclin1 levels in H929 cells at different time points post-transfection. (C) H929 cells (4×10^5 cells/ml) were pretreated with 3-MA (10 mM) for 45 min before the addition of varying concentrations of HYD1. Cell death was determined by FACS analysis of annexin V positive cells after 6 hours of treatment. (n=9; $P<0.05$) (D) H929 cells (4×10^5 cells/ml) were pretreated with 3-MA (10 mM) for 45 min before the addition of 50 μg/ml of HYD1 for 6 hrs and probed for cleaved caspase−3, −9 and −8. Figures shown are a representative of three independent experiments.

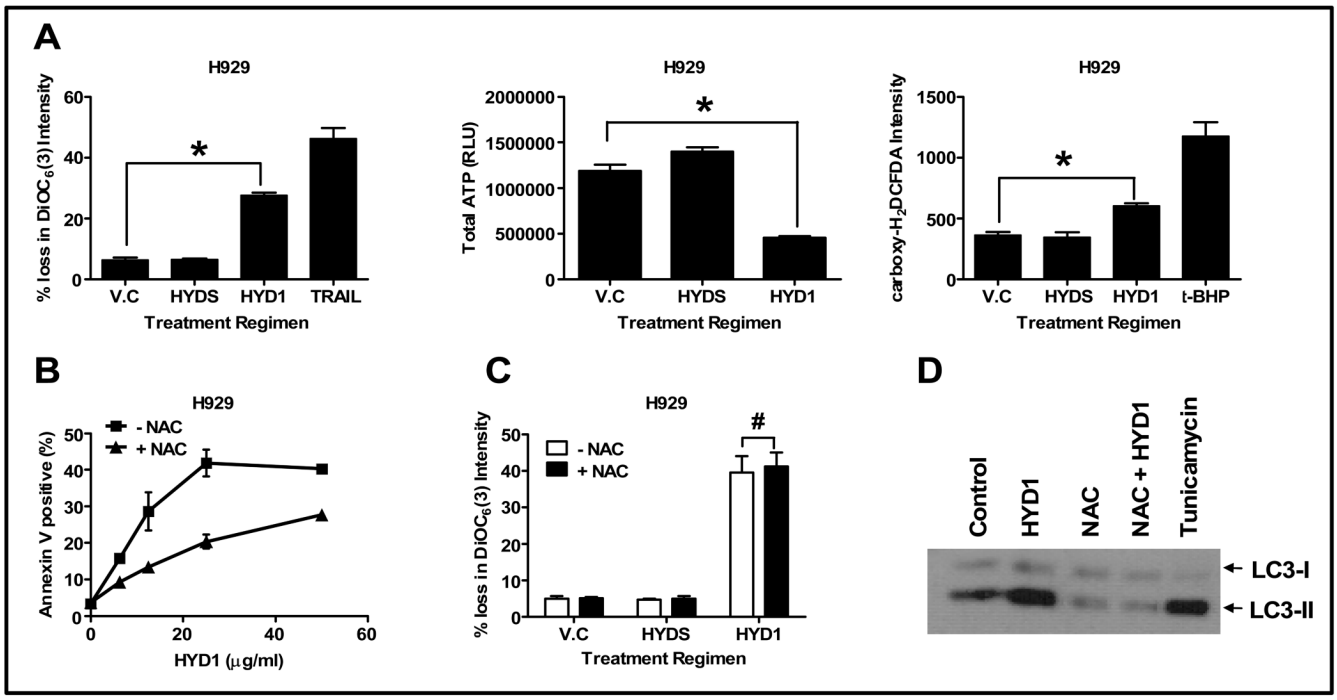

Figure 5. HYD1 induces ROS-mediated necrotic cell death in MM cells

(A) H929 cells (4×10^5 cells/ml) were treated for 2 hrs with HYD1 (50 μg/ml). Following treatment cells were analyzed for loss in $\Delta\psi_m$, total cellular ATP and ROS production as described in the method section (n=9; *, $P<0.05$). (B) Cell death assay was carried out in H929 cells (4×10^5 cells/ml) by pretreating with NAC (10 mM) for 30 min followed by addition of varying concentrations of HYD1 (n=9; $P<0.05$). (C) H929 cells (4×10^5 cells/ml) were pretreated with NAC (10 mM) for 30 min before the addition of HYD1 (50 μg/ml) for an additional 4 hrs. Following the treatment cells were analyzed for loss in $\Delta\psi_m$ (n=9; #, $P>0.05$). (D) H929 cells (4×10^5 cells/ml) were pretreated with NAC (10 mM) for 30 min before the addition of HYD-1 (50 μg/ml) for an additional 4 hrs. Following treatment, the LC3-1 to LC3-II conversion was monitored by western blot analysis. Figures shown are a representative of three independent experiments.

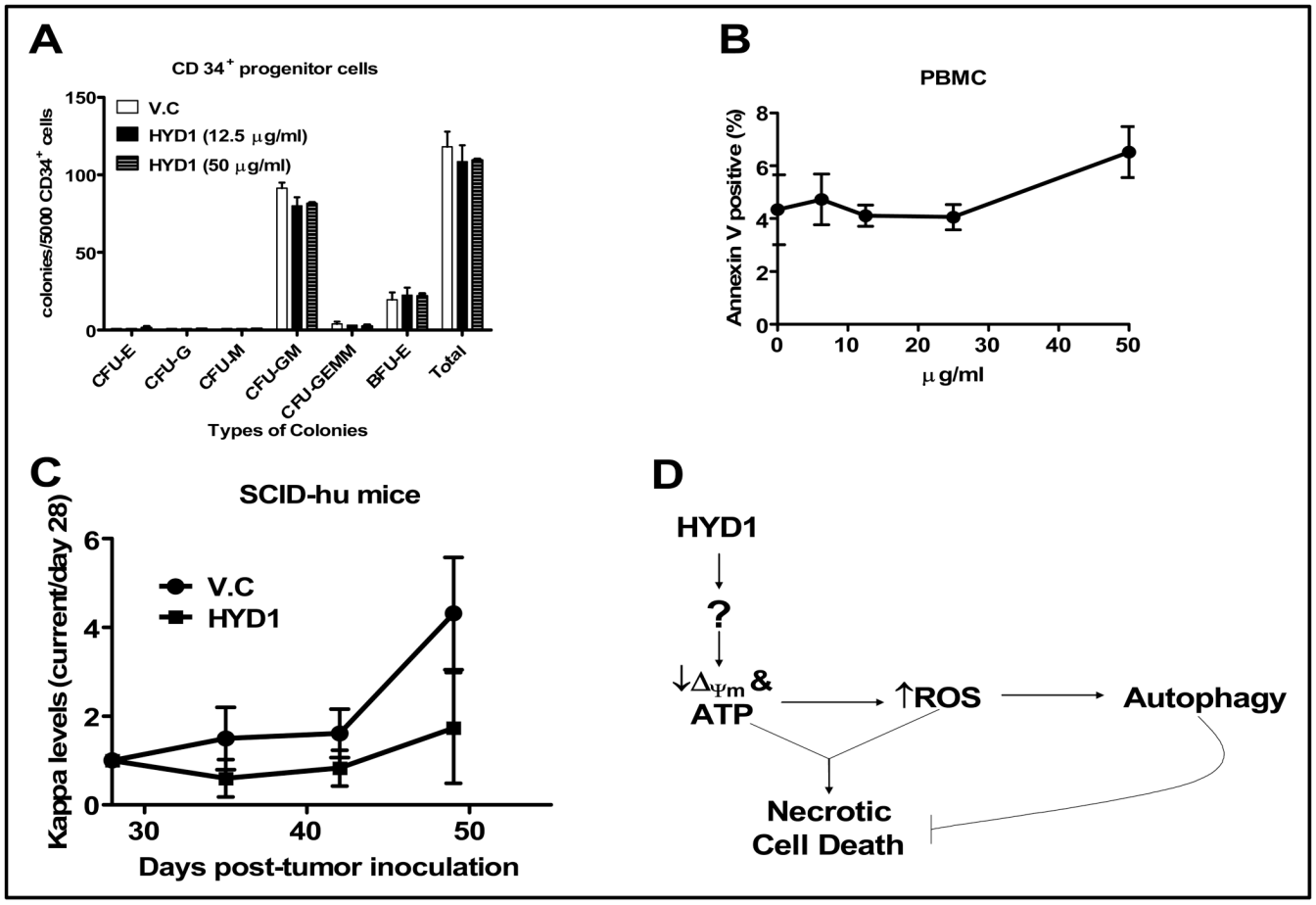

Figure 6. HYD1 lacks activity in normal hematopoietic cells and demonstrates antitumor activity *in vivo*

(A) $CD34^+$ cells were isolated from PBMC of healthy donors and subjected to colony forming assay as described in materials and methods. Number of colonies per 5000 cells was counted at the end of day 12. Experiments were performed twice in duplicates. (B) PBMC were isolated by density gradient centrifugation using Ficoll-Paque. Isolated PBMC (4×10^5 cells/ml) were plated in 24-well plates and treated with the indicated concentrations of HYD1 for 6 hrs followed by measurement of dead cells by FACS analysis of annexin V positive cells. (C) Tumor burden in the SCID-Hu model was measured by circulating kappa levels by ELISA. On day 28 (before drug treatment) measurements were recorded for each individual mouse and subsequent values obtained weekly are represented as a ratio of day 28 (day X/day28). HYD1 was administered i.p. at 8 mg/kg daily for 21 days (starting day 28^{th}). n=5 for vehicle control (V.C) and 4 for HYD1 treated mice ($P<0.05$). (D) A representative model depicting the putative mechanism of action of HYD1 in MM cells.